

# Dual Emissive Manganese and Copper Co-Doped Zn–In–S Quantum Dots as a Single Color-Converter for High Color Rendering White-Light-Emitting Diodes

Xi Yuan,<sup>†</sup> Ruixin Ma,<sup>†</sup> Wenjin Zhang,<sup>‡</sup> Jie Hua,<sup>†,§</sup> Xiangdong Meng,<sup>†</sup> Xinhua Zhong,<sup>‡</sup> Jiahua Zhang,<sup>||</sup> Jialong Zhao,<sup>\*,†</sup> and Haibo Li<sup>\*,†,§</sup>

<sup>†</sup>Key Laboratory of Functional Materials Physics and Chemistry of the Ministry of Education, Jilin Normal University, Siping 136000, China

<sup>‡</sup>Institute of Applied Chemistry, East China University of Science and Technology, Shanghai 200237, China

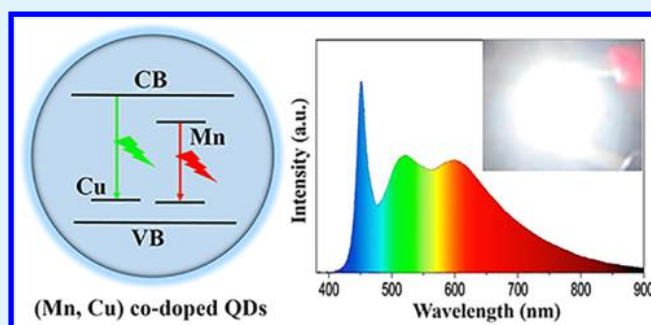
<sup>§</sup>State Key Laboratory of Inorganic Synthesis and Preparative Chemistry, College of Chemistry, Jilin University, Changchun 130012, China

<sup>||</sup>State Key Laboratory of Luminescence and Applications, Changchun Institute of Optics, Fine Mechanics and Physics, Chinese Academy of Sciences, Changchun 130033, China

## Supporting Information

**ABSTRACT:** Novel white light emitting diodes (LEDs) with environmentally friendly dual emissive quantum dots (QDs) as single color-converters are one of the most promising high-quality solid-state lighting sources for meeting the growing global demand for resource sustainability. A facile method was developed for the synthesis of the bright green–red-emitting Mn and Cu codoped Zn–In–S QDs with an absorption bandgap of 2.56 eV (485 nm), a large Stokes shift of 150 nm, and high emission quantum yield up to 75%, which were suitable for warm white LEDs based on blue GaN chips. The wide photoluminescence (PL) spectra composed of Cu-related green and Mn-related red emissions in the codoped QDs could be controlled by varying the doping concentrations of Mn and Cu ions. The energy transfer processes in Mn and Cu codoped QDs were proposed on the basis of the changes in PL intensity and lifetime measured by means of steady-state and time-resolved PL spectra. By integrating these bicolor QDs with commercial GaN-based blue LEDs, the as-fabricated tricolor white LEDs showed bright natural white light with a color rendering index of 95, luminous efficacy of 73.2 lm/W, and color temperature of 5092 K. These results indicated that (Mn,Cu):Zn–In–S/ZnS QDs could be used as a single color-converting material for the next generation of solid-state lighting.

**KEYWORDS:** white light emitting diodes, (Mn,Cu) co-doped quantum dots, quantum dots, energy transfer, nanocrystals



## 1. INTRODUCTION

Environmentally friendly and high-quality white light emitting diodes (LEDs) are very promising to replace traditional light sources for minimizing the artificial lighting globally consumes.<sup>1–4</sup> Present white LEDs integrated yellow-emitting YAG:Ce<sup>3+</sup> phosphors with GaN-based blue-emitting LEDs exhibited low color rendering index (CRI) below 80 due to the deficient red emission<sup>5</sup> and limited luminous efficacy as a result of the severe scattering effect of micrometer-sized phosphors.<sup>6</sup>

Scattering-free/less luminescent semiconductor quantum dots (QDs) as next-generation color converters exhibit size- and composition-dependent photoluminescence (PL), compatibility with solution processing techniques, and high PL quantum yields (QYs) compared to traditional phosphors.<sup>7–11</sup>

The high color rendering white LEDs have been successfully fabricated by using blue or ultraviolet LEDs topped with the

mixture of blue, green, and red light-emitting QDs.<sup>1,12–18</sup> For instance, the mixed red and green CdSe (CuInS<sub>2</sub>) QDs on blue LEDs were used to prepare high-quality white LEDs with luminous efficacy of ~70 lm/W and CRI of 95.<sup>14,17,18</sup> However, the QD mixture often exhibits re-absorption, subsequent undesired energy transfer, and nonuniform luminescent properties, giving rise to the reduction of luminous efficacy and the time-dependent color shift.<sup>1,5,19,20</sup> Hence, single-phase QDs with broad emissions, such as dual emissive ultrasmall CdSe or CdS QDs,<sup>21–25</sup> have been used in white LEDs to avoid the drawback of QD mixture. Yet, the workhorses of color converters, such as Cd-based QDs, have a restricted future due

Received: January 30, 2015

Accepted: April 13, 2015

Published: April 13, 2015

to the severe self-absorption caused by small Stokes shifts of intrinsic CdSe or CdS QDs and the toxicity of heavy metal cadmium.<sup>17,18,26</sup> Therefore, it is necessary to develop low-toxicity QDs with broad emissions as single color-converters for white LED applications.

Transition metal ion doped QDs have been regarded as one of the promising color-converting materials for white LEDs due to their unique features, such as large Stokes shifts, broad PL emissions, and excellent thermal and chemical stability.<sup>27–32</sup> To date, Mn and Cu-doped QDs remained the workhorse, where the Mn ion has a narrow yellow–red emission range of 570–610 nm, while the Cu ion provides host bandgap-dependent wide range tunable emission from blue to near-infrared.<sup>18,19,28,33</sup> Therefore, if both Mn and Cu dopants were doped into the same one-semiconductor nanocrystal, the green–red bicolor QDs are likely to be achieved. In fact, Mn and Cu codoped ZnSe, ZnSeS, and ZnCdS QDs have been successfully prepared.<sup>19,30</sup> These dual-doped QDs showed green–orange or blue–orange bicolor emissions, but no red emission was achieved. Besides, the dual-doped QDs could not be excited effectively by blue light from GaN-based LEDs to achieve white light due to the wide bandgap of semiconductors such as ZnSe, ZnSeS, and ZnCdS QDs above 2.75 eV (450 nm). Additionally, Mn and Cu dopants were introduced at different stages of the host growth, respectively, which make the synthetic process complex and difficult to control.<sup>19,30</sup> Therefore, it is necessary to develop a kind of luminescent QD exhibiting both green and red emissions with high emission efficiency, facile synthetic method, and effective absorption of blue light for fabricating white LEDs with the integration of blue GaN-based LEDs.

Ternary Zn–In–S QDs possess well-developed synthetic approach, composition-tunable band gap, and high chemical stability, which make Zn–In–S a near-ideal host material for doping.<sup>34–36</sup> In this work, by a facile one-pot noninjection method, a new class of Mn and Cu codoped Zn–In–S ((Mn,Cu):Zn–In–S) QD has been synthesized. Heating all the reactants loaded into a reaction flask at room temperature, the Mn and Cu codoped QDs could be obtained, and they exhibited a broad spectral range with two PL peaks at green and red spectral region, respectively. After coating the ZnS shell layer, the highest PL QY of the (Mn,Cu):Zn–In–S/ZnS core/shell QDs could reach up to 75%. The effect of Mn/Cu doping ratio on the spectral shape of broadband emission was studied in detail. The energy transfer processes in Mn and Cu codoped QDs were revealed with time-resolved PL spectroscopy. For solid-state lighting application, high CRI up to 95 and high luminous efficacy of 73.2 lm/W were achieved for the Mn and Cu codoped QD-based white LEDs under excitation of a blue GaN chip by using the single-phase color-converting materials.

## 2. EXPERIMENTAL SECTION

**2.1. Materials.** Sulfur powder (S, 99.99%), indium acetate ( $\text{In}(\text{OAc})_3$ , 99.99%), manganese acetate ( $\text{Mn}(\text{OAc})_2$ , 99.99%), copper acetate ( $\text{Cu}(\text{OAc})_2$ , 99.99%), zinc acetate ( $\text{Zn}(\text{OAc})_2$ , 99.99%), 1-octadecene (ODE, 90%), oleylamine (OAm, 97%), and dodecanethiol (DDT, 99.9%) were purchased from Aldrich. No further purification was provided for all chemicals.

**2.2. Synthesis of (Mn,Cu):Zn–In–S Core.** The (Mn,Cu):Zn–In–S core were synthesized by a one-pot noninjection method. Typically, sulfur powder (0.8 mmol),  $\text{In}(\text{OAc})_3$  (0.2 mmol),  $\text{Zn}(\text{OAc})_2$  (0.2 mmol),  $\text{Cu}(\text{OAc})_2$  (0.02 mmol), and  $\text{Mn}(\text{OAc})_2$  (0.008 mmol) were mixed with OAm (6.0 mL) and DDT (4.0 mL) in a 50 mL flask. Then, the temperature of the mixture solution was

raised to 220 °C (heating rate, 15 °C/min), under argon flow. The reaction solution was kept at 220 °C for 10 min to allow (Mn,Cu):Zn–In–S QD growth. Then, the resulting colloidal solution was cooled to 60 °C, and toluene (10 mL) was added into the reaction mixture. With the addition of excess methanol, the as-prepared QDs precipitated. Repeated centrifugation and decantation were carried out to purify the (Mn,Cu):Zn–In–S core QDs.

**2.3. Growth of ZnS Shell Layer on (Mn,Cu):Zn–In–S Core.** After the crude reaction mixture of (Mn,Cu):Zn–In–S core was maintained at 220 °C for 10 min, the reaction system temperature was cooled to about 100 °C, and then the Zn precursor (dissolving  $\text{Zn}(\text{OAc})_2$  (0.4 mmol) in ODE (0.9 mL) and OAm (0.1 mL)) was injected into the reaction solution. Subsequently, for the overgrowth of ZnS shell, the mixture solution was heated to 240 °C (heating rate of 15 °C/min), and the temperature was maintained at 240 °C for 20 min. The (Mn,Cu):Zn–In–S/ZnS core/shell QD purification progress was similar to the core QD purification described above.

**2.4. Device Fabrication.** A solution (3 mL) of (Mn,Cu):Zn–In–S/ZnS QD (33–66 mg/mL) in chloroform was added into silicone resin (0.3 g, 150 epoxy pouring sealant A; Ausbond, China). The mixed solution was vigorously stirred until homogeneous and heated in vacuum for 1 h at 50 °C to remove the solvent. Then, the (Mn,Cu):Zn–In–S/ZnS QDs and silicone resin composite were further mixed with the hardener (150 epoxy pouring sealant B, 0.15 g) and vigorously stirred until homogeneous. To eliminate any air bubbles, the mixture was heated in a vacuum oven at 50 °C for 30 min. For the fabrication of (Mn,Cu):Zn–In–S/ZnS QD-based white LEDs, the mixture of (Mn,Cu):Zn–In–S/ZnS QDs/silicone resin was dispersed on a GaN-based blue-emitting LED (luminous efficacy of 30 lm/W at 20 mA; Sanan Optoelectronics, China). The obtained white LED was put into a vacuum oven at 100 °C for 30 min. Subsequently, the temperature was increased to 150 °C for 1 h.

**2.5. Characterization.** A Shimadzu UV-2450 UV–vis spectrophotometer was used to record UV–vis absorption spectra. A Horiba Jobin Yvon Fluorolog-3 with a time-correlated single-photon counting (TCSPC) spectrometer and a QY accessory was used to measure the steady-state PL spectra, time-resolved PL spectra, and PL QY. A 150 W ozone-free xenon arc-lamp was utilized as the continuous excitation source. The excitation source for time-resolved PL spectrum measurement was a pulsed xenon lamp or a NanoLED (N-405L or N-300). A Tecnai G2 transmission electron microscope (TEM) operated at 200 kV was utilized to measure the size and shape of the QDs. A Siemens D5005 X-ray powder diffractometer with a  $\text{Cu K}\alpha$  radiation of 1.5406 Å was utilized to record the X-ray diffraction (XRD) spectra. Samples for XRD were prepared via drop-casting QDs onto silicon wafer. A JEOL JSM-7800F scanning electron microscope with an energy dispersive X-ray spectrometer was used to analyze the element composition of the inorganic QDs. Thermo Fisher ESCALAB 250XL photoelectron spectroscopy was used to perform the X-ray photoelectron spectroscopy (XPS) analysis. An Ocean Optics USB4000 spectrometer was utilized to measure the optical properties of the obtained white LEDs.

## 3. RESULTS AND DISCUSSION

The (Mn,Cu):Zn–In–S QDs were synthesized by a one-pot noninjection method via loading sulfur powder and metal acetate salts mixed with OAm and DDT into a reaction flask. After the mixture was heated, Mn and Cu codoped QDs could be obtained. This facile noninjection method was developed from our previous work,<sup>36</sup> featuring scale-up capability and high reproducibility.<sup>36,37</sup> Figure 1 shows UV–visible absorption and PL spectra of the as-obtained (Mn,Cu):Zn–In–S core QDs. The QDs were prepared under the same Cu/(Zn+In) precursor molar ratio of 5% and various Mn/(Zn+In) precursor molar ratios from 1 to 5%. As seen in Figure 1a, a broad absorption band is observed around 400 nm, which is ascribed to the Zn–In–S host excitonic transition.<sup>36</sup> The absorption spectra showed a poorly resolved excitonic absorption feature,

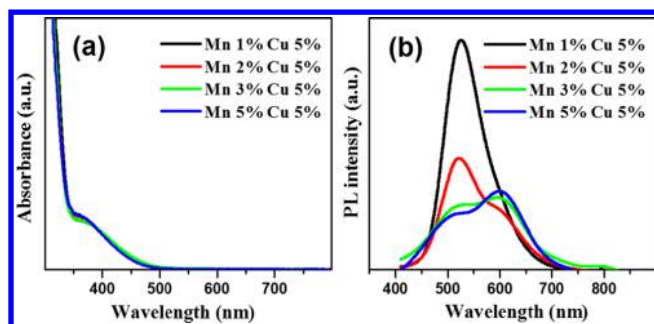


**Figure 1.** (a) UV-visible absorption and (b) PL spectra ( $\lambda_{\text{ex}} = 365$  nm) of (Mn,Cu):Zn-In-S core QDs dispersed in chloroform prepared under the same Cu/(Zn+In) precursor molar ratio of 5% and various Mn/(Zn+In) precursor molar ratios from 1 to 5%.

which related to the intraband gap states, inhomogeneous composition distribution, or both.<sup>38</sup> The wavelength of absorption edge for the QD samples is determined to be 485 nm; thus, the samples can be excited effectively by blue light from GaN-based LEDs. Both the absorption spectral shape and peak position exhibit no variation for the four samples, which indicates that their host QDs possess the coincident particle size and chemical composition. The Mn and Cu codoped QDs show a broad spectral range with two emission peaks located at 523 and 607 nm, respectively, as seen in Figure 1b. The PL band peaked at 523 nm corresponds to Cu ion-related emission, because the Cu-doped Zn-In-S QDs (Zn/In ratio of 1/1, the same for codoped QDs) show the PL peak at about 523 nm (Figure S1, Supporting Information). The PL band peaked at 607 nm should be Mn-related emission, and the PL intensity enhances with increasing the Mn concentration from 1 to 5%. The PL band peaked at 435 nm is observed in undoped Zn-In-S QDs (Figure S2, Supporting Information), which is not found in Mn and Cu codoped QDs. These Mn and Cu codoped QDs exhibit super large full width at half-maximum (fwhm), reaching  $\sim 190$  nm, and the large spectral coverage may be advantageous to solid-state lighting.<sup>1</sup> Besides, the PL QY of the Mn and Cu codoped core QDs is very high and could reach up to 60%.

To improve emission efficiency and stability of (Mn,Cu):Zn-In-S core QDs, we deposited a ZnS shell on the (Mn,Cu):Zn-In-S core in situ. Because there was excess sulfur source in the core reaction mixture, no additional sulfur was needed for the shell depositing process. Figure 2 shows the TEM images and XRD patterns of the (Mn,Cu):Zn-In-S core

and the derivate (Mn,Cu):Zn-In-S/ZnS core/shell QDs to analyze the morphology and structural characterization. The as-obtained QDs were monodispersed and near-spherical, based on the TEM images. The average diameters of (Mn,Cu):Zn-In-S core and (Mn,Cu):Zn-In-S/ZnS core/shell QDs were estimated to be 2.8 and 7.2 nm, respectively, which suggested that the thickness of the ZnS shell is about 7.1 monolayers.<sup>31,39</sup> As seen in the high-resolution TEM images (Figure 2b, inset), the core/shell QDs show clear lattice fringes, which indicates the highly crystalline nature. Figure 2c shows the wide-angle XRD patterns of the (Mn,Cu):Zn-In-S QDs. The diffraction peaks are located between those for cubic ZnS (JCPDS 77-2100) and  $\text{In}_2\text{S}_3$  (JCPDS 05-0731) materials, which indicates that the codoped QDs have cubic zinc blend structures, and Zn-In-S has an alloy structure. The pattern of diffraction peaks and cubic lattices are maintained as the Mn concentration increases. No diffraction peak from Mn and Cu impurities is observed, which indicates that no phase transformation of the crystal structure has occurred after doping Mn and Cu into alloyed Zn-In-S QD host. To investigate the compositions and chemical states of the as-prepared Mn and Cu codoped Zn-In-S QDs, the typical EDS and XPS analysis were carried out (Figure S3, Supporting Information). The composition of the host QDs is  $\text{ZnIn}_{0.57}\text{S}_{2.33}$ . It is noted that the nominal In/Zn ratio (1/1) is higher than the real values (0.57/1), which may be caused by the difference in the chemical reactivity of Zn and In precursors.<sup>36</sup> Besides, the capping thiol ligands existed on the QD surface may lead to the larger S content. The core levels of S 2p, Zn 2p, In 3d, Cu 2p, and Mn 2p were measured via XPS, and the chemical states of the doped QDs were shown to be  $\text{S}^{2-}$ ,  $\text{Zn}^{2+}$ ,  $\text{In}^{3+}$ ,  $\text{Cu}^+$ , and  $\text{Mn}^{2+}$ , respectively.<sup>29,34</sup>

Absorption and PL spectra of (Mn,Cu):Zn-In-S/ZnS core/shell QDs are shown in Figure 3. After overcoating the ZnS shell on the Mn and Cu codoped Zn-In-S core, no significant effect on the absorption spectra was observed, but the emission properties were improved substantially. The PL QY of (Mn,Cu):Zn-In-S/ZnS QDs with 1, 2, 3, and 5% Mn were enhanced adequately from 60, 45, 38, and 35% to 75, 68, 62, and 54%, respectively, after overcoating of the ZnS shell. In addition, the Mn and Cu codoped Zn-In-S QDs exhibited a large Stokes shift about 150 nm. Further, PL spectra of typical 2% Mn and 5% Cu codoped QDs in chloroform and resin film were almost the same; no red shift was observed (Figure S4, Supporting Information), suggesting that no energy transfer progress occurred in the codoped QD films. To understand

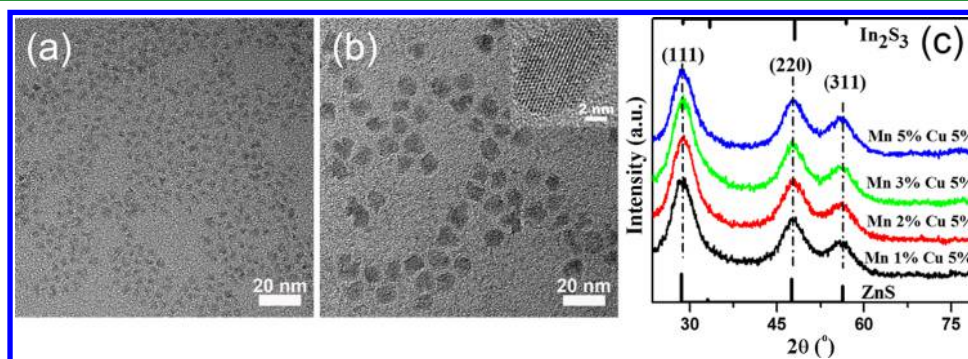


**Figure 2.** TEM images of (a) (Mn,Cu):Zn-In-S (2% Mn and 5% Cu) core QDs and (b) the derivate (Mn,Cu):Zn-In-S/ZnS core/shell QDs. (c) XRD patterns of (Mn,Cu):Zn-In-S core QDs with different Mn concentration. The XRD patterns for bulk  $\text{In}_2\text{S}_3$  (top, JCPDS 05-0731) and ZnS (bottom, JCPDS 77-2100) are shown as reference.

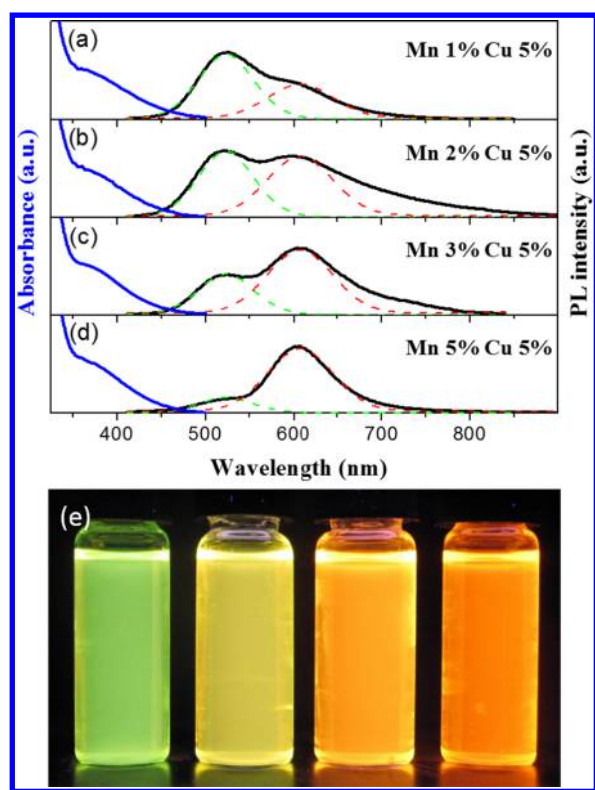


**Figure 3.** (a–d, blue lines) UV–visible absorption and (black lines) PL spectra of (Mn,Cu):Zn–In–S/ZnS core/shell QDs with a fixed Cu concentration of 5% and variable Mn concentrations from 1 to 5%, respectively. The individual emissions of Mn and Cu ions are also presented by green and red dashed lines, respectively. (e) Digital picture of the QD samples under the radiation of a UV lamp.

these issues, we calculated spectral overlap ( $J$ ) with the following equation:<sup>40</sup>

$$J = \int_0^{\infty} F_D(\lambda) \varepsilon_A(\lambda) \lambda^4 d\lambda \quad (1)$$

where  $F_D(\lambda)$  is the normalized donor emission spectrum, and  $\varepsilon_A(\lambda)$  is acceptor absorption spectrum. The value of overlap integral  $J$  of (Mn,Cu):Zn–In–S/ZnS QDs are  $3.754 \times 10^{14}$  (1% Mn and 5% Cu),  $3.536 \times 10^{14}$  (2% Mn and 5% Cu),  $2.167 \times 10^{14}$  (3% Mn and 5% Cu), and  $1.052 \times 10^{14}$  (5% Mn and 5% Cu)  $M^{-1} \text{ cm}^{-1} \text{ nm}^4$ , respectively, which are much smaller than that of classical CdSe QDs ( $3.434 \times 10^{16} M^{-1} \text{ cm}^{-1} \text{ nm}^4$ ).<sup>18</sup> The considerable difference (about 2 orders of magnitude) indicates that the self-absorption and energy transfer in Mn and Cu codoped QD ensembles could be negligible,<sup>40</sup> which are beneficial to the efficiency of white LEDs based on them.

Each Mn and Cu codoped QD PL spectrum can be decomposed into two emission bands via fitting of a Gaussian function, showing two peaks located in 523 and 607 nm with widths of 75 and 91 nm for Cu and Mn ions, respectively, as seen in Figure 3a–d. The emission at the long wavelength range (above 650 nm), not included in the fitting curves, may be attributed to defect emission.<sup>41,42</sup> As the Mn concentration increases, the Cu ion emission decreases, followed by the enhancement of Mn ion emission, which may be attributed to energy gain competition between Mn and Cu dopant from Zn–In–S host, energy transfer from Cu to Mn ions doped in Zn–In–S host, or both. The enhancement of Mn emission changes the spectral shape of the QDs from green-emitting (1%

Mn) to the orange-emitting (5% Mn) gradually, as seen in Figure 3e. Then, the white light could be generated via a combination of the tuned yellow-emitting QDs and the blue-emitting LEDs.

Figure 4 shows the PL decay curves of the (Mn,Cu):Zn–In–S/ZnS core/shell QDs. Multiexponential decay function was

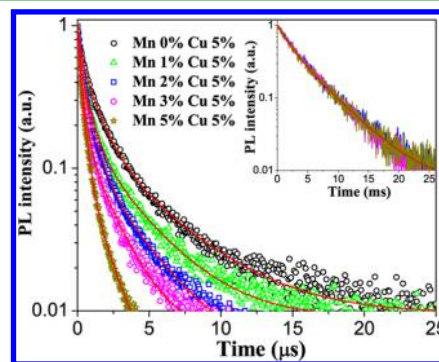


**Figure 4.** Time-resolved PL decay curves of (Mn,Cu):Zn–In–S/ZnS core/shell QDs with a fixed Cu concentration of 5% and variable Mn concentrations from 0 to 5%, respectively, measured at 523 nm. (Inset) Mn-related PL decay curve of the (Mn,Cu):Zn–In–S/ZnS core/shell QDs, measured at 607 nm. The solid red lines represent fitting curves.

employed to analyze the PL decays. The average lifetime was defined as follows:<sup>40</sup>

$$\tau_{av} = \int_0^{\infty} I(t) dt \quad (2)$$

where  $I(t)$  is the normalized initial intensity of PL at time  $t$ . Table 1 lists the obtained PL lifetimes. The PL lifetimes monitored at 523 nm were in the range of about 0.38–1.33 μs, which was consistent with the excited-state lifetime of Cu dopant emission, several microseconds or hundred-nanoseconds, owing to the recombination radiation between the hole in Cu  $T_2$  and the electron in the host conduction band.<sup>26,36</sup> Besides, the PL lifetime monitoring at 607 nm was measured to be about 3.909 ms, which is comparable to that of ZnS:Mn QDs,<sup>39</sup> owing to  ${}^4T_1-{}^6A_1$  transition of the Mn ions,<sup>19,28</sup> indicating that Mn ions were effectively doped in the QDs. This confirms that the green emission is related to the Cu dopant and the red one originates from the Mn dopant. On the other hand, the lifetime of the Mn ion-related PL is 3 or 4 orders of magnitude longer than that of the green light, which means their PL decay measurements can be distinguished from each other, though there is some spectral overlap between them.

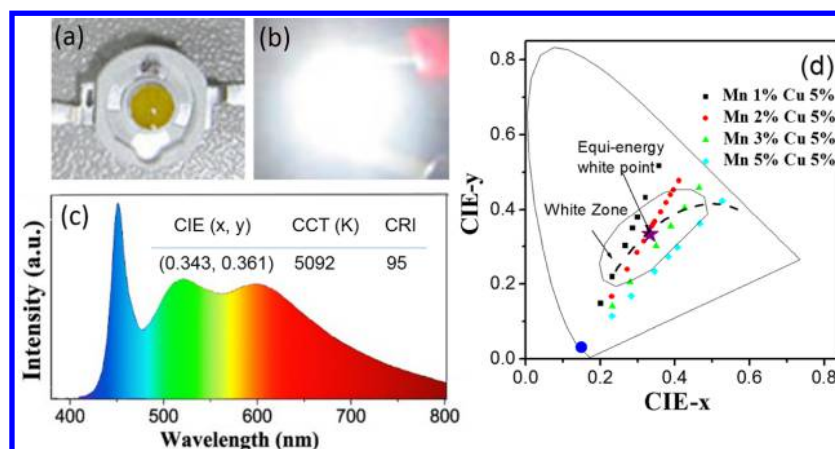
The decays of Cu ion-related PL speed up (Figure 4), and the corresponding PL lifetimes are reduced greatly (Table 1) as the Mn concentration increases from 0 to 5%, accompanied by a decrease in the intensity ratio of Cu ion related emission to Mn ion emission. This indicates that energy transfer could take place from Cu to Mn ions, because energy transfer is an additional de-excitation channels for donors, expressed as  $1/\tau_{DA} = 1/\tau_D + k_{ET}$ , where  $\tau_{DA}$  and  $\tau_D$  are PL lifetimes for Cu donor with and without Mn ions in QDs,  $k_{ET}$  is energy transfer rate. Energy transfer efficiency ( $\eta_{ET}$ ) can be calculated by<sup>40</sup>

$$\eta_{ET} = 1 - \tau_{DA}/\tau_D \quad (3)$$

Both the  $\eta_{ET}$  and  $k_{ET}$  are also summarized in Table 1. The energy transfer efficiency  $\eta_{ET}$  increases with increasing the Mn

**Table 1.** Lifetimes of Mn and Cu Ion-Related PL in (Mn,Cu):Zn–In–S/ZnS QDs with Fixed Cu Concentration and Variable Mn Concentrations, as well as the Energy Transfer Efficiency and Rate from Cu to Mn Ions

samples	Mn 0%, Cu 5%	Mn 1%, Cu 5%	Mn 2%, Cu 5%	Mn 3%, Cu 5%	Mn 5%, Cu 5%
$\tau_{av}$ -Cu ( $\mu$ s)	1.32	0.89	0.78	0.52	0.38
$\tau_{av}$ -Mn (ms)		3.89	3.91	3.90	3.91
$\eta_{ET}$ (%)		32.61	40.96	60.05	71.28
$k_{ET}$ ( $s^{-1}$ )		$3.64 \times 10^5$	$5.23 \times 10^5$	$1.13 \times 10^6$	$1.87 \times 10^6$

**Figure 5.** Digital images of the as-fabricated white LED based on single type of (Mn,Cu):Zn–In–S/ZnS QDs under (a) zero current and (b) forward current of 20 mA. (c) EL spectrum of the device operated at 20 mA. (d) CIE color coordinates of the devices with various concentrations of the QDs in the silicone resin. The black dashed line represents the blackbody locus curve.

concentration and reaches 71% for 5% Mn-doped QD sample. Otherwise, the PL lifetimes for Mn ions are especially long and nearly unchanged with increasing the Mn concentration, which suggests that there is no concentration self-quenching within the range of Mn concentrations in the series of samples. Generally, assuming that there is no energy gain competition between Mn and Cu dopant from Zn–In–S host, it is true for the following expression  $I_{DA}/I_D = \tau_{DA}/\tau_D$ , where  $I_{DA}$  and  $I_D$  are the PL intensity of Cu donor with and without Mn ion in the QDs, respectively.<sup>43,44</sup> In particular, the quenching ratio of  $\tau_{DA}/\tau_D$  (0.67, 0.59, 0.39, and 0.28 for 1, 2, 3, and 5% Mn-doped QD samples, respectively) is larger than  $I_{DA}/I_D$  (0.61, 0.44, 0.25, and 0.12 for 1, 2, 3, and 5% Mn-doped QD samples, respectively), depending on the concentration of Mn dopants. Therefore, the energy gain competition between Mn and Cu dopants from Zn–In–S host presents in codoped QDs. We ascertain that the relative quenching contributions of (1) energy gain competition between Mn and Cu dopants from Zn–In–S host and (2) energy transfer from Cu to Mn ions can be described by a relation  $I_{DA}/I_D = (N_{DA}/N_D) \times (\tau_{DA}/\tau_D)$ , where  $N_{DA}$  and  $N_D$  are assumed Cu-related emitting centers in presence and absence of Mn ion. The values of  $N_{DA}/N_D$  are 0.90, 0.74, 0.65, and 0.42 for 1, 2, 3, and 5% Mn-doped QD samples, respectively, which suggests that the excitation energy of Mn ion from the ZnCuInS host increases with increasing the Mn ion concentration, which is in agreement with the increase of energy transfer rate from host to Mn dopants as the doping concentration of Mn ions increases.<sup>45</sup>

The white LEDs can be fabricated via combination of the Mn and Cu codoped Zn–In–S QDs with the blue GaN LEDs. Figure 5a shows the as-fabricated white LED that integrates a blue (450 nm) emitting LED chip with single type of Mn and Cu codoped QDs (2% Mn and 5% Cu). The picture of the white LED operating at 20 mA is shown in Figure 5b. The single QD-converting white LED emits bright natural white

light with CIE color coordinate of (0.34, 0.36), CRI value up to 95, correlated color temperature (CCT) of 5092 K, close to sun light, and luminous efficacy of 73.2 lm/W (Table 2). The

**Table 2.** CRI, Luminous Efficacy (LE), CCT, and CIE Color Coordinates of the As-Fabricated White LEDs based on (Mn,Cu):Zn–In–S/ZnS QDs Operated at 20 mA

sample	CRI	LE (lm/W)	CCT (K)	CIE (x,y)
Mn 1%, Cu 5%	79	62.7	7700	(0.29, 0.35)
Mn 2%, Cu 5%	95	73.2	5092	(0.34, 0.36)
Mn 3%, Cu 5%	87	44.5	4487	(0.35, 0.30)
Mn 5%, Cu 5%	66	37.6	2716	(0.38, 0.27)

performance is much better than that reported previously in literature for QD-based white LEDs using blends of two or three kinds of CdSe QDs (luminous efficacy of 41 lm/W, CIE of (0.24, 0.21)).<sup>14</sup> Apparently, the enhanced device performance can be attributed to the high emission efficiency of (Mn,Cu):Zn–In–S/ZnS QDs and no reabsorption and subsequent undesired energy transfer induced energy loss due to using single emitter as color-converting material. Besides, the CRI of the white LEDs based on Cu-doped QDs (single type, CRI < 75)<sup>18</sup> is lower than that based on Mn and Cu codoped QDs (single type, CRI of 95). For enhancing the CRI, CCT, and luminous efficacy could reach 95, 5198 K, and 74.7 lm/W, respectively, comparable to those of Mn and Cu codoped QDs.<sup>18</sup> However, a single type of emitter as color-converting material provides many advantages over multiple-component ones, such as simpler fabrication processes, greater reproducibility, ease of modification, and low-cost preparation, as well as effectively restraint of the undesirable chromaticity coordinate variations caused by various relatively temporal stabilities for different QDs.<sup>19</sup> It is also noted that the white

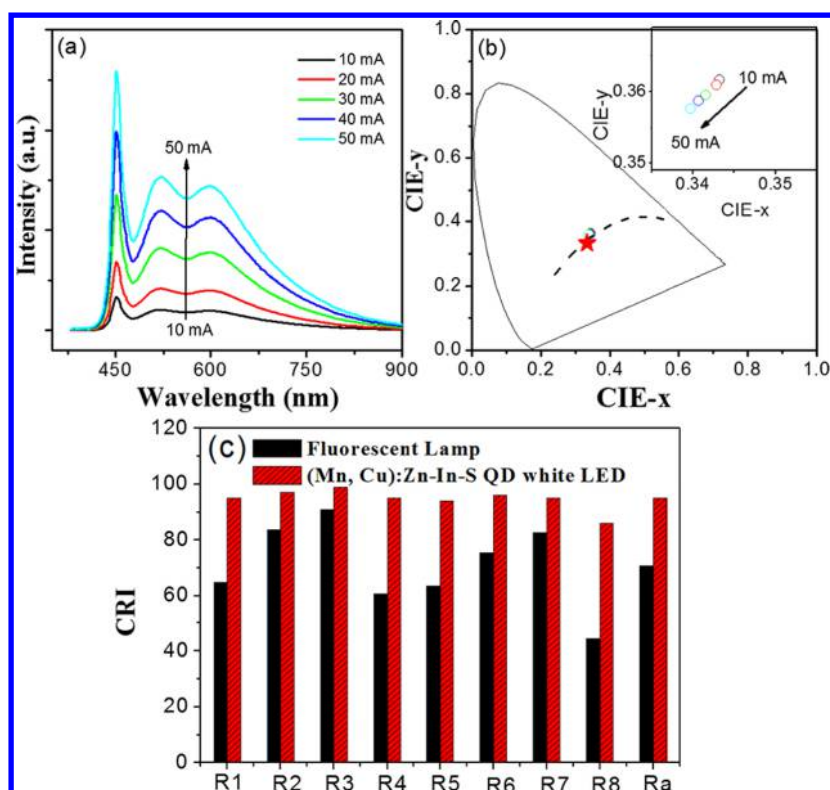


**Figure 6.** (a) EL spectra of a white LED fabricated with (Mn,Cu):Zn-In-S/ZnS QDs (2% Mn and 5% Cu) as a function of forward current from 10 to 50 mA. (b) CIE color coordinates of the as-fabricated white LED under different forward bias currents. The black dashed line represents the blackbody locus curve. (c) CRI of the fluorescent lamp (Panasonic YZ18RR6500K) and (Mn,Cu):Zn-In-S/ZnS QD white LED operated at 20 mA.

LEDs based on single type of undoped QDs reported in literature show low CRI (<80),<sup>17,46,47</sup> such as the ZnSe, CdSe, and CuInS<sub>2</sub> QDs, because their luminescences are not wide enough. To solve this problem, many groups integrated the band-edge emission with the broad surface-state emissions to generate a broad emission.<sup>21,48,49</sup> However, surface-state emissions showed poor stability and low PL efficiency, which make the device performance undesirable. However, the electroluminescence (EL) spectrum of the as-fabricated single emitter-converted white LED based on (Mn,Cu):Zn-In-S/ZnS QDs covers a broad spectral region from 420 to 800 nm, as seen in Figure 5c. Three distinct peaks are clearly observed and refer to GaN LED blue light (450 nm), Cu-related green light (523 nm), and Mn-related red light (607 nm), respectively. These make (Mn,Cu):Zn-In-S/ZnS QDs promising for white LED application. As seen in Figure 5d, the CIE color coordinates of white LEDs can cover the white light range via tuning concentrations of QDs in resin, corresponding typical EL spectrum for 1, 3, and 5% Mn ion doped samples, which are shown in Figure S5 (Supporting Information). The CIE coordinates of the white LEDs exhibit a nearly linear increase with increasing the QD concentration, the corresponding slopes monotonously reduce from 2.36 to 1.04 with increasing the Mn amount of the QDs from 1 to 5%. These lines provide a guide for white LED design.

Table 2 gives the device parameters of typical white LEDs based on (Mn,Cu):Zn-In-S/ZnS QDs operated at a driving current of 20 mA. The CRI values for the white LEDs based on 2 and 3% Mn ion doped QD samples are over 85, which can satisfy the requirements for indoor illumination (CRI > 80). The highest luminous efficacy of white LEDs could reach up to

73.2 lm/W, which is the best value for white LEDs based only on single type of QDs, when the CRI value is over 90. The CCT values show a very broad region of 2716–7700 K, which exhibits a decreasing trend as the Mn-related emission is enhanced. This indicates that the Mn and Cu codoped Zn-In-S QDs are promising color converters for white LEDs.

Figure 6a shows EL spectra for the white LEDs based on (Mn,Cu):Zn-In-S/ZnS QDs (2% Mn and 5% Cu) at different forward currents. The emission intensity of the QDs increased with enhancing the forward current from 10 to 50 mA, which suggests that the (Mn,Cu):Zn-In-S/ZnS QDs exhibit no saturation. As seen in Figure 6b, under different forward bias currents, the corresponding color coordinates of the as-fabricated LED exhibit little change, which indicates that the white LED possesses good color stability. The little shift of the color coordinates to the blue side could be ascribed to the thermally quenched emission of QDs, because the temperature of LED chips increase with increasing the forward current.<sup>50</sup> Figure 6c shows the detailed CRI values (R1–R8) and the average value (Ra) of R1–R8 for fluorescent lamp (Panasonic YZ18RR6500K) and white LED based on (Mn,Cu):Zn-In-S/ZnS QDs (2% Mn) operated at 20 mA. The QD-based white LED shows a much higher Ra of 95 and improvements of color reproduction from R1 to R8, in comparison with the Ra value of 71 for fluorescent lamp. These results show that white light generated from the (Mn,Cu):Zn-In-S/ZnS QD-converted white LED has excellent color reproducibility.

#### 4. CONCLUSION

In summary, we have fabricated highly bright white LEDs based on bicolor (Mn,Cu):Zn-In-S/ZnS core/shell QDs with the

PL QY of 75% under excitation of blue GaN chips for the next generation of solid-state lighting. Mn and Cu codoped QDs with two emission peaks located at 523 and 607 nm were prepared by a facile one-pot noninjection method. With steady-state and time-resolved PL spectroscopy, we demonstrated that the green emission peak originated from the Cu-related emission, and the red one was related to the  ${}^4T_1-{}^6A_1$  transition of Mn ions. The intensity ratio of the red/green emissions could be tailored by varying the doping concentration of Mn and Cu ions, which is probably controlled via energy transfer in Mn and Cu codoped QDs. The optimized white LEDs based on blue GaN chips and green–red-emitting (Mn,Cu):Zn–In–S/ZnS QDs showed high CRI of 95, CCT of 2716–7700 K, and luminous efficacy up to 73.2 lm/W, which are the best values of white LEDs only based on single type QDs, currently reported. The achievement of tricolor (blue/green/red) white LEDs with a single type of dual emissive Mn and Cu codoped Zn–In–S QDs instead of combination of two types of single-color QDs make the low toxic (Mn,Cu):Zn–In–S QDs promising for manufacturing high color rendering white LEDs with high efficacy.

## ■ ASSOCIATED CONTENT

### ■ Supporting Information

UV–visible absorption and PL spectra of Cu:Zn–In–S QDs; PL spectra of undoped Zn–In–S QDs; EDS pattern and XPS spectra of (Mn,Cu):Zn–In–S/ZnS QDs; PL spectra of (Mn,Cu):Zn–In–S QDs (2% Mn and 5% Cu) in chloroform solution and resin film; EL spectra of the white LEDs based on (Mn,Cu):Zn–In–S/ZnS QDs with a fixed Cu concentration of 5% and variable Mn concentrations from 1 to 5%. This material is available free of charge via the Internet at <http://pubs.acs.org>.

## ■ AUTHOR INFORMATION

### ■ Corresponding Authors

\*Phone: +86-434-3290232. E-mail: [lihaibo@jlnu.edu.cn](mailto:lihaibo@jlnu.edu.cn).

\*Phone: +86-431-81765161. E-mail: [zhaojl@jlnu.edu.cn](mailto:zhaojl@jlnu.edu.cn).

### ■ Notes

The authors declare no competing financial interest.

## ■ ACKNOWLEDGMENTS

This work was supported by the National Natural Science Foundation of China (Nos. 11274304, 21371071, and 61275047) and the Research Project of Chinese Ministry of Education (No. 213009A).

## ■ REFERENCES

- (1) Dai, Q.; Duty, C. E.; Hu, M. Z. Semiconductor Nanocrystals Based White Light-Emitting Diodes. *Small* **2010**, *6*, 1577–1588.
- (2) Li, X.; Budai, J. D.; Liu, F.; Howe, J. Y.; Zhang, J.; Wang, X.-J.; Gu, Z.; Sun, C.; Meltzer, R. S.; Pan, Z. New Yellow  $Ba_{0.93}Eu_{0.07}Al_2O_4$  Phosphor for Warm-White Light-Emitting Diodes through Single-Emitting-Center Conversion. *Light: Sci. Appl.* **2013**, *2*, e50.
- (3) Nakamura, S.; Mukai, T.; Senoh, M. Candela-Class High-Brightness InGaN/AlGaIn Double-Heterostructure Blue-Light-Emitting Diodes. *Appl. Phys. Lett.* **1994**, *64*, 1687–1689.
- (4) Schubert, E. F.; Kim, J. K. Solid-State Light Sources Getting Smart. *Science* **2005**, *308*, 1274–1278.
- (5) Liu, Y.; Zhang, X.; Hao, Z.; Wang, X.; Zhang, J. Generation of Broadband Emission by Incorporating  $N^{3-}$  into  $Ca_3Sc_2Si_3O_{12}:Ce^{3+}$  Garnet for High Rendering White LEDs. *J. Mater. Chem.* **2011**, *21*, 6354–6358.

- (6) Cosgun, A.; Fu, R.; Jiang, W.; Li, J.; Song, J.; Song, X.; Zeng, H. Flexible Quantum Dot–PVA Composites for White LEDs. *J. Mater. Chem. C* **2015**, *3*, 257–264.

- (7) Coe, S.; Woo, W.-K.; Bawendi, M.; Bulović, V. Electroluminescence from Single Monolayers of Nanocrystals in Molecular Organic Devices. *Nature* **2002**, *420*, 800–803.

- (8) Dohnalová, K.; Poddubny, A. N.; Prokofiev, A. A.; de Boer, W. D.; Umesh, C. P.; Paulusse, J. M.; Zuillhof, H.; Gregorkiewicz, T. Surface Brightens up Si Quantum Dots: Direct Bandgap-like Size-Tunable Emission. *Light: Sci. Appl.* **2013**, *2*, e47.

- (9) Colvin, V.; Schlamp, M.; Alivisatos, A. Light-Emitting Diodes Made from Cadmium Selenide Nanocrystals and a Semiconducting Polymer. *Nature* **1994**, *370*, 354–357.

- (10) Tessler, N.; Medvedev, V.; Kazes, M.; Kan, S.; Banin, U. Efficient Near-Infrared Polymer Nanocrystal Light-Emitting Diodes. *Science* **2002**, *295*, 1506–1508.

- (11) Chuang, P.-H.; Lin, C. C.; Liu, R.-S. Emission-Tunable  $CuInS_2/ZnS$  Quantum Dots: Structure, Optical Properties, and Application in White Light-Emitting Diodes with High Color Rendering Index. *ACS Appl. Mater. Interfaces* **2014**, *6*, 15379–15387.

- (12) Jun, S.; Lee, J.; Jang, E. Highly Luminescent and Photostable Quantum Dot–Silica Monolith and Its Application to Light-Emitting Diodes. *ACS Nano* **2013**, *7*, 1472–1477.

- (13) Chen, H.-S.; Hong, H.-Y.; Kumar, R. V. White Light Emission from Semiconductor Nanocrystals by in Situ Colour Tuning in an Alternating Thermodynamic–Kinetic Fashion. *J. Mater. Chem.* **2011**, *21*, 5928–5932.

- (14) Jang, E.; Jun, S.; Jang, H.; Lim, J.; Kim, B.; Kim, Y. White-Light-Emitting Diodes with Quantum Dot Color Converters for Display Backlights. *Adv. Mater.* **2010**, *22*, 3076–3080.

- (15) Wang, X.; Li, W.; Sun, K. Stable Efficient CdSe/CdS/ZnS Core/Multishell Nanophosphors Fabricated through a Phosphine-Free Route for White Light-Emitting-Diodes with High Color Rendering Properties. *J. Mater. Chem.* **2011**, *21*, 8558–8565.

- (16) Demir, H. V.; Nizamoglu, S.; Erdem, T.; Mutlugun, E.; Gaponik, N.; Eychmüller, A. Quantum Dot Integrated LEDs Using Photonic and Excitonic Color Conversion. *Nano Today* **2011**, *6*, 632–647.

- (17) Chen, B.; Zhong, H.; Wang, M.; Liu, R.; Zou, B. Integration of  $CuInS_2$ -Based Nanocrystals for High Efficiency and High Colour Rendering White Light-Emitting Diodes. *Nanoscale* **2013**, *5*, 3514–3519.

- (18) Yuan, X.; Hua, J.; Zeng, R.; Zhu, D.; Ji, W.; Jing, P.; Meng, X.; Zhao, J.; Li, H. Efficient White Light Emitting Diodes Based on Cu-doped ZnInS/ZnS Core/Shell Quantum Dots. *Nanotechnology* **2014**, *25*, 435202.

- (19) Panda, S. K.; Hickey, S. G.; Demir, H. V.; Eychmüller, A. Bright White-Light Emitting Manganese and Copper Co-Doped ZnSe Quantum Dots. *Angew. Chem.* **2011**, *50*, 4432–4436.

- (20) Huang, B.; Dai, Q.; Zhuo, N.; Jiang, Q.; Shi, F.; Wang, H.; Zhang, H.; Liao, C.; Cui, Y.; Zhang, J. Bicolor Mn-Doped  $CuInS_2/ZnS$  Core/Shell Nanocrystals for White Light-Emitting Diode with High Color Rendering Index. *J. Appl. Phys.* **2014**, *116*, 094303.

- (21) Bowers, M. J.; McBride, J. R.; Rosenthal, S. J. White-Light Emission from Magic-Sized Cadmium Selenide Nanocrystals. *J. Am. Chem. Soc.* **2005**, *127*, 15378–15379.

- (22) Schreuder, M. A.; Gosnell, J. D.; Smith, N. J.; Warnement, M. R.; Weiss, S. M.; Rosenthal, S. J. Encapsulated White-Light CdSe Nanocrystals as Nanophosphors for Solid-State Lighting. *J. Mater. Chem.* **2008**, *18*, 970–975.

- (23) Gosnell, J. D.; Rosenthal, S. J.; Weiss, S. M. White Light Emission Characteristics of Polymer-Encapsulated CdSe Nanocrystal Films. *IEEE Photonics Technol. Lett.* **2010**, *22*, 541–543.

- (24) Schreuder, M. A.; Xiao, K.; Ivanov, I. N.; Weiss, S. M.; Rosenthal, S. J. White Light-Emitting Diodes Based on Ultrasmall CdSe Nanocrystal Electroluminescence. *Nano Lett.* **2010**, *10*, 573–576.

- (25) Ozel, T.; Soganci, I. M.; Nizamoglu, S.; Huyal, I. O.; Mutlugun, E.; Sapra, S.; Gaponik, N.; Eychmüller, A.; Demir, H. V. Selective Enhancement of Surface-State Emission and Simultaneous Quenching

of Interband Transition in White-Luminophor CdS Nanocrystals Using Localized Plasmon Coupling. *New J. Phys.* **2008**, *10*, 083035.

(26) Wang, X.; Yan, X.; Li, W.; Sun, K. Doped Quantum Dots for White-Light-Emitting Diodes without Reabsorption of Multiphase Phosphors. *Adv. Mater.* **2012**, *24*, 2742–2747.

(27) Norris, D. J.; Efros, A. L.; Erwin, S. C. Doped Nanocrystals. *Science* **2008**, *319*, 1776–1779.

(28) Pradhan, N.; Goorskey, D.; Thessing, J.; Peng, X. An Alternative of CdSe Nanocrystal Emitters: Pure and Tunable Impurity Emissions in ZnSe Nanocrystals. *J. Am. Chem. Soc.* **2005**, *127*, 17586–17587.

(29) Jishu Han, J.; Zhang, H.; Tang, Y.; Liu, Y.; Yao, X.; Yang, B. Role of Redox Reaction and Electrostatics in Transition-Metal Impurity-Promoted Photoluminescence Evolution of Water-Soluble ZnSe Nanocrystals. *J. Phys. Chem. C* **2009**, *113*, 7503–7510.

(30) Jana, S.; Srivastava, B. B.; Pradhan, N. Correlation of Dopant States and Host Bandgap in Dual-Doped Semiconductor Nanocrystals. *J. Phys. Chem. Lett.* **2011**, *2*, 1747–1752.

(31) Yuan, X.; Zheng, J.; Zeng, R.; Jing, P.; Ji, W.; Zhao, J.; Yang, W.; Li, H. Thermal Stability of Mn<sup>2+</sup> Ion Luminescence in Mn-doped Core-Shell Quantum Dots. *Nanoscale* **2014**, *6*, 300–307.

(32) Cao, S.; Li, C.; Wang, L.; Shang, M.; Wei, G.; Zheng, J.; Yang, W. Long-Lived and Well-Resolved Mn<sup>2+</sup> Ion Emissions in CuInS–ZnS Quantum Dots. *Sci. Rep.* **2014**, *4*, 7510.

(33) Zhang, W.; Zhou, X.; Zhong, X. One-Pot Noninjection Synthesis of Cu-Doped Zn(x)Cd(1-x)S Nanocrystals with Emission Color Tunable over Entire Visible Spectrum. *Inorg. Chem.* **2012**, *51*, 3579–3587.

(34) Chen, Z.; Li, D.; Zhang, W.; Chen, C.; Li, W.; Sun, M.; He, Y.; Fu, X. Low-Temperature and Template-Free Synthesis of ZnIn<sub>2</sub>S<sub>4</sub> Microspheres. *Inorg. Chem.* **2008**, *47*, 9766–9772.

(35) Gou, X.; Cheng, F.; Shi, Y.; Zhang, L.; Peng, S.; Chen, J.; Shen, P. Shape-Controlled Synthesis of Ternary Chalcogenide ZnIn<sub>2</sub>S<sub>4</sub> and CuIn(S,Se)<sub>2</sub> Nano-/Microstructures via Facile Solution Route. *J. Am. Chem. Soc.* **2006**, *128*, 7222–7229.

(36) Zhang, W.; Lou, Q.; Ji, W.; Zhao, J.; Zhong, X. Color-Tunable Highly Bright Photoluminescence of Cadmium-Free Cu-Doped Zn-In-S Nanocrystals and Electroluminescence. *Chem. Mater.* **2014**, *26*, 1204–1212.

(37) Zhang, W.; Zhang, H.; Feng, Y.; Zhong, X. Scalable Single-Step Noninjection Synthesis of High-Quality Core/Shell Quantum Dots with Emission Tunable from Violet to Near-Infrared. *ACS Nano* **2012**, *6*, 11066–11073.

(38) Zhong, X.; Liu, S.; Zhang, Z.; Li, L.; Wei, Z.; Knoll, W. Synthesis of High-Quality CdS, ZnS, and Zn<sub>x</sub>Cd<sub>1-x</sub>S Nanocrystals Using Metal Salts and Elemental Sulfur. *J. Mater. Chem.* **2004**, *14*, 2790–2794.

(39) Zheng, J.; Yuan, X.; Ikezawa, M.; Jing, P.; Liu, X.; Zheng, Z.; Kong, X.; Zhao, J.; Masumoto, Y. Efficient Photoluminescence of Mn<sup>2+</sup> Ions in MnS/ZnS Core/Shell Quantum Dots. *J. Phys. Chem. C* **2009**, *113*, 16969–16974.

(40) Lakowicz, J. R. *Principles of Fluorescence Spectroscopy*. 3rd ed. Springer-Verlag: Berlin, 2006.

(41) Yang, H.; Holloway, P. H. Enhanced Photoluminescence from CdS: Mn/ZnS Core/Shell Quantum Dots. *Appl. Phys. Lett.* **2003**, *82*, 1965–1967.

(42) Nag, A.; Cherian, R.; Mahadevan, P.; Gopal, A. V.; Hazarika, A.; Mohan, A.; Vengurlekar, A.; Sarma, D. Size-Dependent Tuning of Mn<sup>2+</sup> d Emission in Mn<sup>2+</sup>-Doped CdS Nanocrystals: Bulk vs Surface. *J. Phys. Chem. C* **2010**, *114*, 18323–18329.

(43) Carraway, E.; Demas, J.; DeGraff, B. Luminescence Quenching Mechanism for Microheterogeneous Systems. *Anal. Chem.* **1991**, *63*, 332–336.

(44) Carraway, E.; Demas, J.; DeGraff, B.; Bacon, J. Photophysics and Photochemistry of Oxygen Sensors Based on Luminescent Transition-metal Complexes. *Anal. Chem.* **1991**, *63*, 337–342.

(45) Chen, H.-Y.; Maiti, S.; Son, D. H. Doping Location-Dependent Energy Transfer Dynamics in Mn-doped CdS/ZnS Nanocrystals. *ACS Nano* **2012**, *6*, 583–591.

(46) Nizamoglu, S.; Ozel, T.; Sari, E.; Demir, H. White Light Generation Using CdSe/ZnS Core–Shell Nanocrystals Hybridized

with InGaN/GaN Light Emitting Diodes. *Nanotechnology* **2007**, *18*, 065709.

(47) Chung, W.; Park, K.; Yu, H. J.; Kim, J.; Chun, B.-H.; Kim, S. H. White Emission Using Mixtures of CdSe Quantum Dots and PMMA as a Phosphor. *Opt. Mater.* **2010**, *32*, 515–521.

(48) Chen, H. S.; Wang, S. J. J.; Lo, C. J.; Chi, J. Y. White-Light Emission from Organics-Capped ZnSe Quantum Dots and Application in White-Light-Emitting Diodes. *Appl. Phys. Lett.* **2005**, *86*, 131905.

(49) Nag, A.; Sarma, D. White Light from Mn<sup>2+</sup>-doped CdS Nanocrystals: A New Approach. *J. Phys. Chem. C* **2007**, *111*, 13641–13644.

(50) Song, W.-S.; Kim, J.-H.; Lee, J.-H.; Lee, H.-S.; Do, Y. R.; Yang, H. Synthesis of Color-Tunable Cu–In–Ga–S Solid Solution Quantum Dots with High Quantum Yields for Application to White Light-Emitting Diodes. *J. Mater. Chem.* **2012**, *22*, 21901–21908.